Formosa Journal of Science and Technology (FJST)
Vol. 4, No. 4, 2025: 1101-1116

A Grey Relational Analysis Approach to Optimize FDM 3D Printing Parameters Using Open-Source Experimental Data

Sunardi
Department of Mechanical Engineering, Faculty of Engineering, Universitas Muhammadiyah Yogyakarta
Corresponding Author: Sunardi, sunardi@umy.ac.id

ARTICLE INFO

Keywords: Fused Deposition Modeling, 3D Printing, Process Optimization, Gray Relational Analysis, Mechanical Properties

Received : 27, March
Revised : 10, April
Accepted : 27, April

ABSTRACT

This study investigates the optimization of key process parameters in Fused Deposition Modeling (FDM) to enhance surface quality and mechanical properties. Using open-source data from 50 test runs, nine parameters were analyzed. Gray Relational Analysis (GRA) identified the optimal setting—layer height (0.02 mm), wall thickness (9 mm), 70% infill density, grid pattern, 215 °C nozzle, 75 °C bed, 40 mm/s speed, PLA material, and 75% fan speed—with a Gray Relational Grade of 0.8685. This configuration significantly improved surface roughness, tensile strength, and elongation. The findings provide a practical reference for improving FDM performance. Future research should explore advanced materials and multi-objective optimization for broader applicability.

ISSN-E: 2964-6804
DOI: https://doi.org/10.55927/fjst.v4i4.61
https://traformosapublisher.org/index.php/fjst

INTRODUCTION

Additive manufacturing (AM), particularly Fused Deposition Modeling (FDM), has emerged as a widely adopted technique due to its simplicity, cost-effectiveness, and versatility in producing functional parts and prototypes (Kumar et al., 2023). Despite its widespread use, the mechanical performance and surface quality of FDM-printed parts are highly dependent on process parameters such as layer height, wall thickness, infill pattern and density, nozzle and bed temperatures, print speed, material type, and fan speed. Inappropriate parameter settings often lead to defects, including poor surface finish, dimensional inaccuracies, and mechanical failure (Khan et al., 2022).

Recent studies have explored various optimization techniques to improve FDM output quality. Traditional methods such as Taguchi have been applied successfully for parameter tuning (Raju et al., 2022), while data-driven approaches, including machine learning algorithms like genetic algorithms (GA) and artificial neural networks (ANN), offer predictive optimization but often require extensive datasets and complex modeling (Lee et al., 2019; Tamir et al., 2023). In contrast, Gray Relational Analysis (GRA) has gained popularity as a robust and computationally efficient method for multi-objective optimization, particularly when experimental data is limited (Chakraborty et al., 2023).

Several recent works have demonstrated GRA’s effectiveness in enhancing surface roughness, tensile strength, and dimensional accuracy in FDM applications (Kumar et al., 2024; Molero et al., 2020). However, many focus on isolated parameters, lacking a holistic approach that captures the interaction effects among multiple variables. To address this, the present study combines GRA with a structured Taguchi experimental design to evaluate nine critical parameters simultaneously, enabling a more integrated optimization framework.

The contribution of this study lies in its methodological integration of GRA and Taguchi design to optimize FDM performance based on open-source experimental data. This approach not only enriches the literature by offering a simplified yet effective optimization strategy but also provides actionable insights for researchers and practitioners aiming to enhance print reliability and quality.

THEORETICAL REVIEW

Fused Deposition Modelling and Process Parameters

Fused Deposition Modeling (FDM) is a widely adopted additive manufacturing process that fabricates parts layer-by-layer using thermoplastic filaments. Key process parameters such as layer height, wall thickness, infill density, infill pattern, nozzle and bed temperatures, print speed, material type, and fan speed significantly influence the final part quality (Kechagias & Zaoutsos, 2024; Kumar et al., 2023). Surface roughness, tensile strength, dimensional accuracy, and build time are sensitive to these settings. For example, lower layer height typically improves surface finish but increases print duration, while denser infill enhances mechanical strength at the cost of material usage(Dev & Srivastava, 2021).

Gray Relational Analysis (GRA)

Gray Relational Analysis (GRA) is a decision-making method based on Gray System Theory, designed to handle systems with limited and uncertain information (Chen, 2023). In the context of FDM, GRA has been successfully used to optimize multiple conflicting outputs such as minimizing surface roughness while maximizing tensile strength and dimensional accuracy by evaluating the relational grade among experimental outcomes (Chakraborty et al., 2023). When combined with Taguchi's orthogonal arrays, GRA provides a streamlined yet powerful approach to parameter optimization without requiring intensive computation (Patel et al., 2024).

METHODOLOGY

Data Collection

The dataset used in this study was obtained from an open-source database on Kaggle (www.kaggle.com/afumetto/3dprinter). This dataset contains various records of 3D printer input parameters and corresponding output performance metrics, such as surface roughness (µm), elongation (%), and tensile strength (MPa). The dataset provides valuable insights into the relationships between key printing parameters, enabling data-driven optimization.

The dataset comprises 50 experimental runs with variations in critical Fused Deposition Modeling (FDM) process parameters, including layer height (mm), wall thickness (mm), infill density (%), infill pattern (grid, honeycomb), nozzle temperature (ºC), bed temperature (ºC), print speed (mm/s), material (ABS, PLA), and fan speed (%). These parameters significantly influence the quality and mechanical properties of the printed components.

This study utilizes Gray Relational Analysis (GRA) to identify optimal process conditions. The structured dataset facilitates systematic exploration of parameter interactions, supporting data-driven optimization to enhance print quality and mechanical performance. Furthermore, the use of open-source data ensures reproducibility and enables comparative studies in FDM-based 3D printing optimization.

To evaluate print quality, nine key input parameters were analyzed, along with three performance indicators surface roughness (µm), tensile strength (MPa), and elongation (%) which assess structural integrity, surface smoothness, and mechanical properties. By systematically varying these parameters and measuring their impact, this study aims to determine the optimal combination for improving overall print quality. Tables 1 and 2 present the input and output parameters along with their measurement symbols and units.

Table 1. Configurations of input parameters used in the 3D printing process

Input parameters	Units
Layer height	mm
Wall thickness	mm
Infill density	%

Infill pattern	Grid, Honeycomb
Nozzle temperature	ºC
Bed temperature	ºC
Print speed	mm/s
Material	ABS, PLA
Fan speed	%

Table 2. Output parameters measured for 3D printed product quality

Output parameters	**Units**
Surface Roughness	µm
Tension strength	Mpa
Elongation	%

Based on open-source data from Kaggle, the values of nine process parameters were obtained, including layer height (a), wall thickness (b), infill density (c), infill pattern (d), nozzle temperature (e), bed temperature (f), print speed (g), material type (h), and fan speed (i), each evaluated at multiple levels. The layer height varied across five levels: 0.02 mm (Level 1), 0.06 mm (Level 2), 0.1 mm (Level 3), 0.15 mm (Level 4), and 0.2 mm (Level 5). Wall thickness was set within a range of 1–10 mm, while infill density varied between 10% and 90%. The infill pattern was selected as either a grid or honeycomb structure. The nozzle temperature was tested at 200 ºC, 205 ºC, 210 ºC, 215 ºC, 220 ºC, 225 ºC, 230 ºC, 240 ºC, and 250 ºC. The bed temperature was adjusted across five levels: 60 ºC, 65 ºC, 70 ºC, 75 ºC, and 80 ºC. Print speed was evaluated at 40 mm/s, 60 mm/s, and 120 mm/s, while fan speed was varied at 0%, 25%, 50%, and 100%. The thermoplastic filament materials used in this study were Acrylonitrile Butadiene Styrene (ABS) and Polylactic Acid (PLA), selected based on their relevance to additive manufacturing processes. The output parameters measured included surface roughness (Ra) in µm, tensile strength (TS) in MPa, and elongation (E) in %. Table 3 presents the relationship between the input parameter settings and the corresponding output results.

Table 3. Dataset used to analyses the correlation between 3D printer input parameters

Run No.	**Setting Input Parameters**									**Output Parameters**		
	(a)	***(b)***	***(c)***	***(d)***	***(e)***	***(f)***	***(g)***	***(h)***	***(i)***	***(Ra)***	***(TS)***	***(E)***
1	0.02	8	90	grid	220	60	40	ABS	0	25	18	1.2
2	0.02	7	90	honeycomb	225	65	40	ABS	25	32	16	1.4
3	0.02	1	80	grid	230	70	40	ABS	50	40	8	0.8
4	0.02	4	70	honeycomb	240	75	40	ABS	75	68	10	0.5
5	0.02	6	90	grid	250	80	40	ABS	100	92	5	0.7
6	0.02	10	40	honeycomb	200	60	40	PLA	0	60	24	1.1
7	0.02	5	10	grid	205	65	40	PLA	25	55	12	1.3
8	0.02	10	10	honeycomb	210	70	40	PLA	50	21	14	1.5
9	0.02	9	70	grid	215	75	40	PLA	75	24	27	1.4
10	0.02	8	40	honeycomb	220	80	40	PLA	100	30	25	1.7

11	0.06	6	80	grid	220	60	60	ABS	0	75	37	2.4
12	0.06	2	20	honeycomb	225	65	60	ABS	25	92	12	1.4
13	0.06	10	50	grid	230	70	60	ABS	50	118	16	1.3
14	0.06	6	10	honeycomb	240	75	60	ABS	75	200	9	0.8
15	0.06	3	50	grid	250	80	60	ABS	100	220	10	1
16	0.06	10	90	honeycomb	200	60	60	PLA	0	126	27	2.2
17	0.06	3	40	grid	205	65	60	PLA	25	145	23	1.9
18	0.06	8	30	honeycomb	210	70	60	PLA	50	88	26	1.6
19	0.06	5	80	grid	215	75	60	PLA	75	92	33	2.1
20	0.06	10	50	honeycomb	220	80	60	PLA	100	74	29	2
21	0.1	1	40	grid	220	60	120	ABS	0	120	16	1.2
22	0.1	2	30	honeycomb	225	65	120	ABS	25	144	12	1.1
23	0.1	1	50	grid	230	70	120	ABS	50	265	10	0.9
24	0.1	9	80	honeycomb	240	75	120	ABS	75	312	19	0.8
25	0.1	2	60	grid	250	80	120	ABS	100	368	8	0.4
26	0.1	1	50	honeycomb	200	60	120	PLA	0	180	11	1.6
27	0.1	4	40	grid	205	65	120	PLA	25	176	12	1.2
28	0.1	3	50	honeycomb	210	70	120	PLA	50	128	18	1.8
29	0.1	4	90	grid	215	75	120	PLA	75	138	34	2.9
30	0.1	1	30	honeycomb	220	80	120	PLA	100	121	14	1.5
31	0.15	4	50	grid	220	60	60	ABS	0	168	27	2.4
32	0.15	7	10	honeycomb	225	65	60	ABS	25	154	19	1.8
33	0.15	6	50	grid	230	70	60	ABS	50	225	18	1.4
34	0.15	1	50	honeycomb	240	75	60	ABS	75	289	9	0.6
35	0.15	7	80	grid	250	80	60	ABS	100	326	13	0.7
36	0.15	3	80	honeycomb	200	60	60	PLA	0	192	33	2.8
37	0.15	4	50	grid	205	65	60	PLA	25	212	24	1.8
38	0.15	10	30	honeycomb	210	70	60	PLA	50	168	26	2.1
39	0.15	6	40	grid	215	75	60	PLA	75	172	22	2.3
40	0.15	1	10	honeycomb	220	80	60	PLA	100	163	4	0.7
41	0.2	4	80	grid	220	60	40	ABS	0	212	35	3.3
42	0.2	9	90	honeycomb	225	65	40	ABS	25	276	34	3.1
43	0.2	7	30	grid	230	70	40	ABS	50	298	28	2.2
44	0.2	6	90	honeycomb	240	75	40	ABS	75	360	28	1.6
45	0.2	3	80	grid	250	80	40	ABS	100	357	21	1.1
46	0.2	5	60	honeycomb	200	60	40	PLA	0	321	28	2.7
47	0.2	4	20	grid	205	65	40	PLA	25	265	14	1.8
48	0.2	5	60	honeycomb	210	70	40	PLA	50	278	30	3.2
49	0.2	7	40	grid	215	75	40	PLA	75	244	29	3.2
50	0.2	3	60	honeycomb	220	80	40	PLA	100	220	27	3.1

Relational Methodology Using Grey Relational Analysis

To examine the combined influence of several process parameters on the resulting properties of parts produced through Fused Deposition Modeling (FDM), a multi-criteria decision-making framework was implemented using Grey Relational Analysis (GRA). This approach is suitable for handling systems characterized by limited or incomplete information and enables quantitative evaluation of relationships among various experimental outcomes.

Step 1: Construction of Experimental Data Matrix

Experimental results from multiple test runs are structured into a two-dimensional array where each row corresponds to a specific experimental configuration and each column represents a particular performance attribute. The general form of this matrix is defined as:

$$X = \begin{bmatrix} x_0(1) & x_o(2) & \cdots & x_0(k) \\ x_1(1) & x_1(2) & \cdots & x_1(k) \\ \vdots & \vdots & \vdots & \vdots \\ x_n(1) & x_n(2) & \cdots & x_n(k) \end{bmatrix} \text{...(1)}$$

Here, $x_i(k)$ denotes the k^{th} response value in the i^{th} experiment, where $i = 0,1,\ldots,n$ and $k = 1,2,\ldots,m$.

Step 2: Data Normalization

To enable direct comparison between attributes with different physical scales, each column of the data matrix is normalized using one of three standard transformation rules, depending on the desired performance direction:

Data normalization is carried out by selecting one of the normalization methods, namely:

- Larger-is-Better:

$$x_i^*(k) = \frac{x_i(k) - min\,(x_i(k))}{max\,(x_i(k)) - min\,(x_i(k))} \text{...(2)}$$

- Smaller-is-Better:

$$x_i^*(k) = \frac{max\,(x_i(k)) - x_i(k)}{max\,(x_i(k)) - min\,(x_i(k))} \text{..(3)}$$

- Nominal-is-Best:

$$x_i^*(k) = \frac{x_i\,(k)}{x_i\,(1)} \text{..(4)}$$

These transformations ensure that the normalized values fall within the interval [0, 1], facilitating further analysis.

Step 3: Computation of Deviation Sequences.

The degree of deviation for each observation from the ideal reference sequence (usually the first experimental run) is calculated as:

$$\Delta_i(k) = |x_0^*(k) - x_i^*(k)| \text{..(5)}$$

Subsequently, the global minimum ($\Delta_{\min}$) and maximum (Δ_{max}) deviations across all entries are determined as:

$$\Delta_{min} = \frac{min}{i,k} \Delta_i(k),\ \Delta_{max} = \frac{max}{i,k} \Delta_i(k) \quad \text{..}(6)$$

Step 4: Gray Relational Coefficients Calculation

To quantify the relative proximity of each experimental response to the ideal case, the Grey Relational Coefficient (GRC) is derived using:

$$\gamma_i(k) = \frac{\Delta_{min} + \xi \cdot \Delta_{max}}{\Delta_i(k) + \xi \cdot \Delta_{max}} \quad \text{...}(7)$$

The distinguishing coefficient ξ, which controls the contrast of relational coefficients, is typically assigned a value of 0.5 to reflect moderate distinguishing sensitivity.

Step 5: Gray Relational Grade Aggregation

The Grey Relational Grade (GRG) for each experiment is computed as the arithmetic mean of its corresponding GRCs:

$$GRG_i = \frac{1}{m} \sum_{k=1}^{m} \gamma_i(k) \quad \text{..}\ (8)$$

This score encapsulates the overall desirability of the parameter setting by aggregating its performance across multiple quality characteristics.

Step 6: Optimal Parameter Determination

Finally, the experimental configurations are ranked based on their GRG values. The experiment that achieves the highest grade is deemed to represent the most effective combination of process parameters under the selected criteria. This ranking aids in identifying optimal settings for improving the functional attributes of FDM-printed components.

RESEARCH RESULTS

This study investigates the influence of key 3D printing process parameters layer height, fan speed, print speed, material type, bed temperature, infill pattern, nozzle temperature, infill density, and wall thickness on the resulting surface roughness (Ra), tensile strength (TS), and elongation (E) of printed components. The experimental results are visualized in Figures 1–9 and summarized through gray relational analysis (GRA) in Table 4.

The analysis reveals that:

1. Layer height is positively correlated with surface roughness and elongation, while tensile strength improves after a certain threshold (Figure 1).

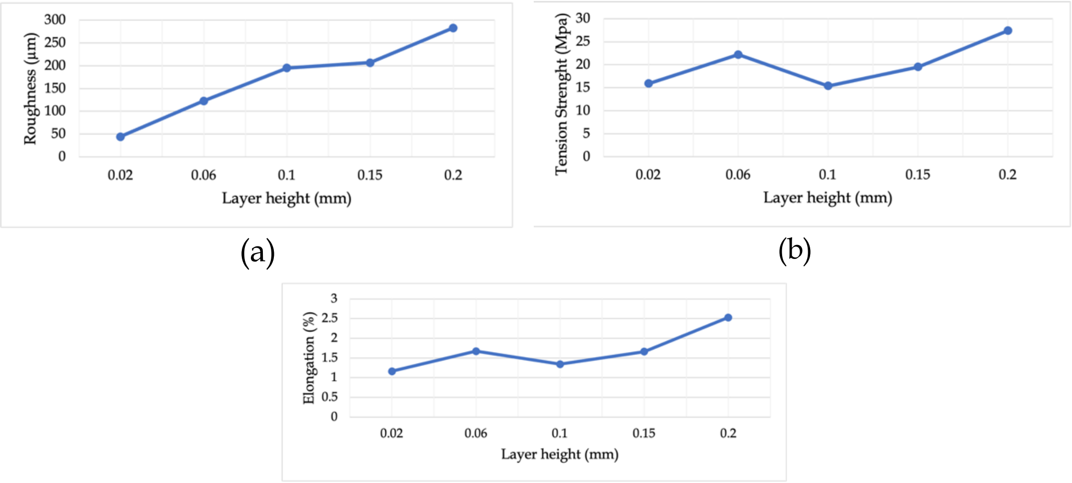

(a) (b)

(c)

Figure 1. Effect of layer height on (a) surface roughness, (b) tensile strength and (c) elongation

2. Fan speed has a negative impact on both tensile strength and elongation, with a slight increase in surface roughness (Figure 2).

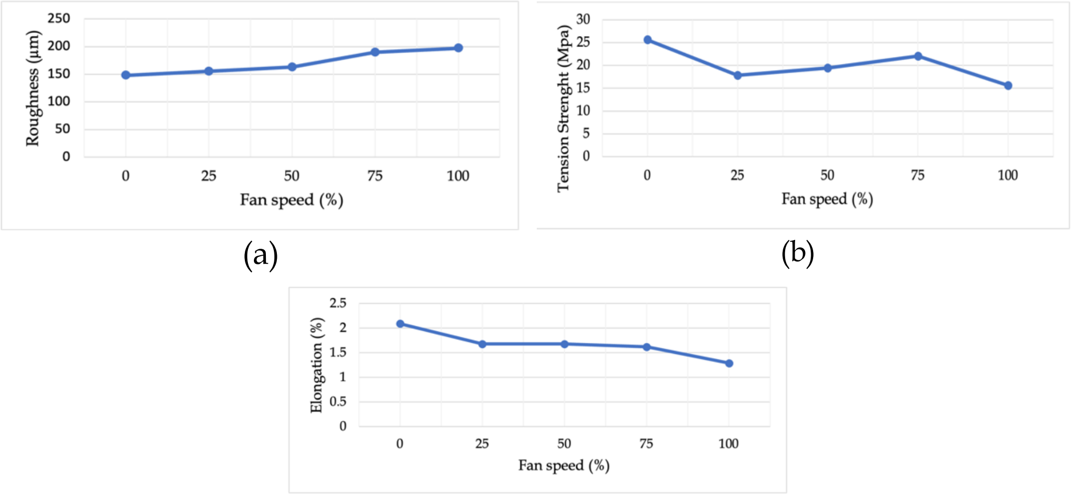

(a) (b)

(c)

Figure 2. Effect of fan speed on (a) surface roughness, (b) tensile strength and (c) elongation

3. Print speed affects all output parameters adversely at higher values; surface roughness increases while both tensile strength and elongation decline (Figure 3).

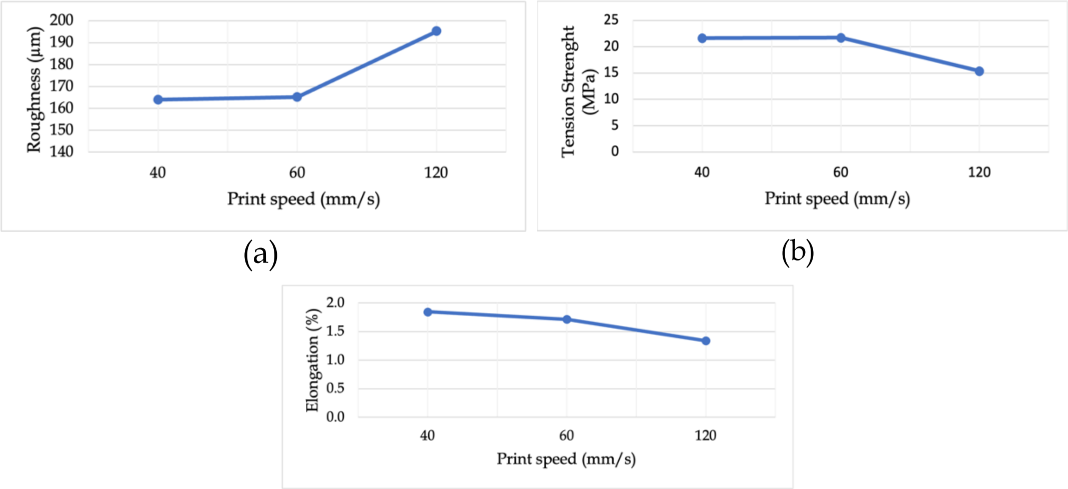

(a) (b)

(c)

Figure 3. Effect of print speed on (a) surface roughness, (b) tensile strength and (c) elongation

4. Material type shows PLA outperforming ABS in all measured aspects: smoother surface, higher tensile strength, and better ductility (Figure 4).

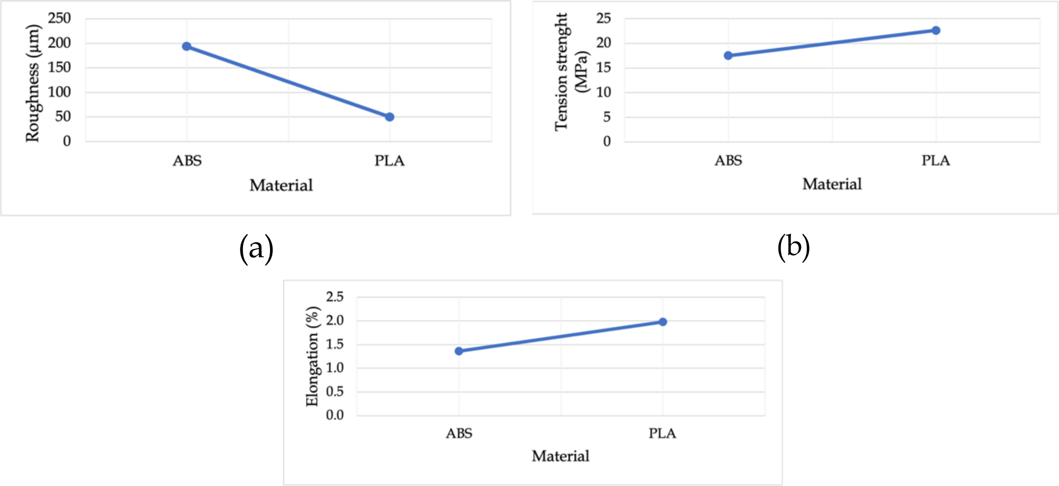

(a) (b)

(c)

Figure 4. Effect of material on (a) surface roughness, (b) tensile strength and (c) elongation

5. Bed temperature elevation results in degraded mechanical properties and increased surface roughness (Figure 5).

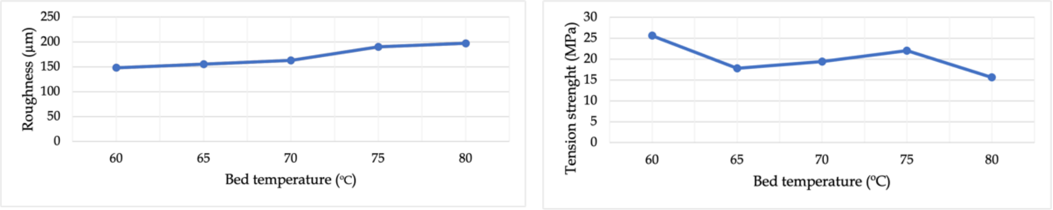

(a) (b)

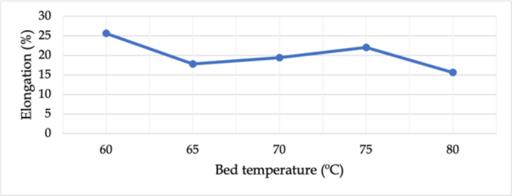

(c)

Figure 5. Effect of bed temperature on (a) surface roughness (b) tensile strength and (c) elongation

6. Infill pattern influences mechanical strength and surface quality, with the honeycomb pattern yielding superior results compared to the grid (Figure 6).

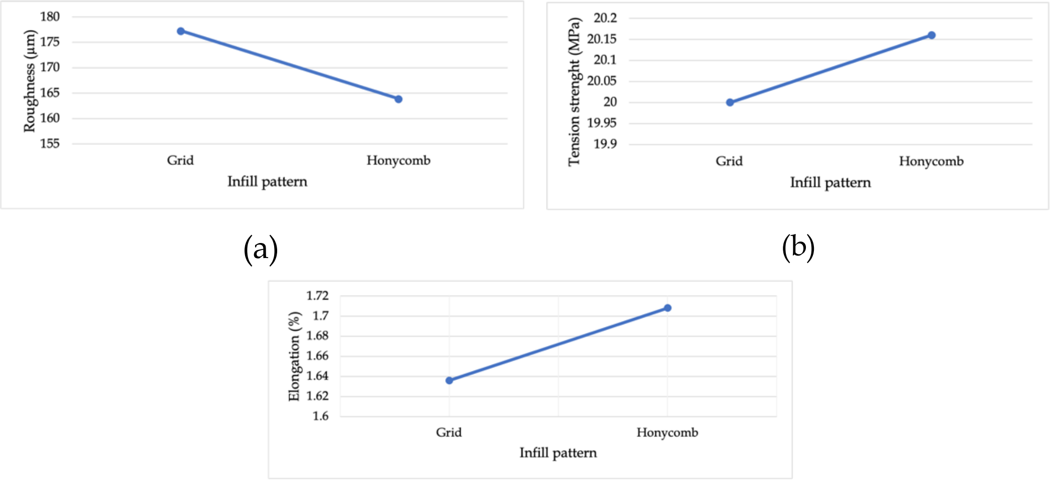

(a) (b)

(c)

Figure 6. Effect of infill pattern on (a) surface roughness (b) tensile strength and (c) elongation

7. Nozzle temperature exhibits an optimal range (215–220°C) beyond which both mechanical properties and surface finish deteriorate (Figure 7).

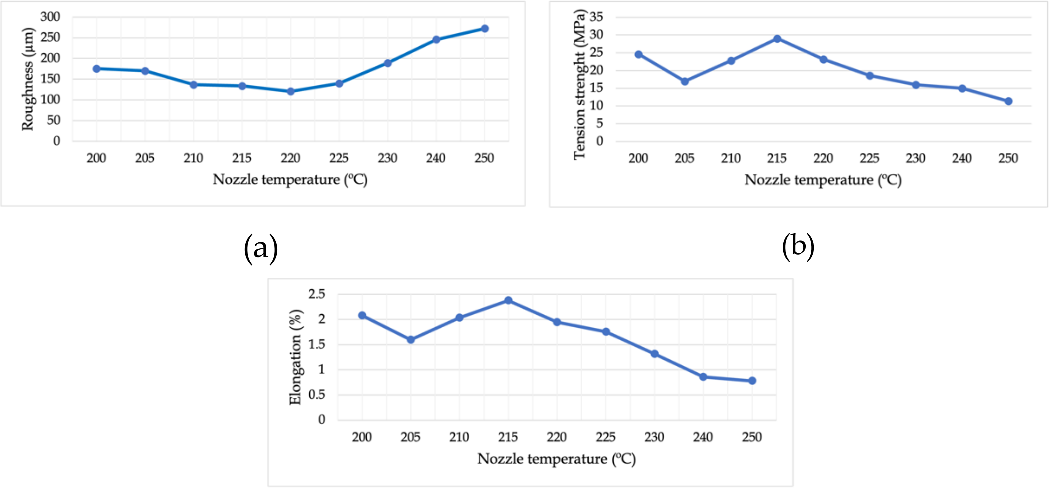

(a) (b)

(c)

Figure 7. Effect of nozzle temperature on (a) surface roughness (b) tensile strength and (c) elongation

8. Infill density shows a non-linear relationship; optimal surface quality occurs around 40–50%, with tensile strength increasing moderately and elongation remaining relatively stable (Figure 8).

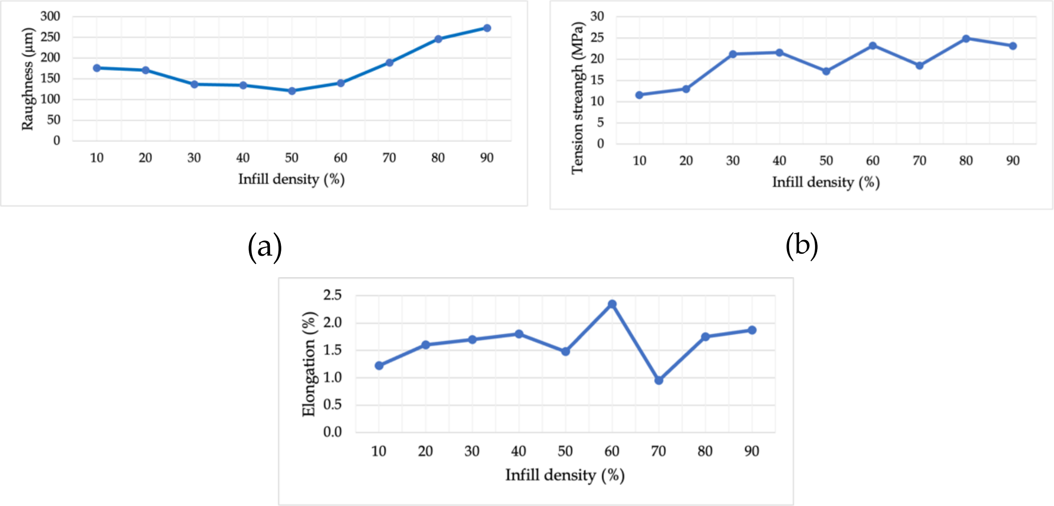

(a)

(b)

(c)

Figure 8. Effect of infill density on (a) surface roughness (b) tensile strength and (c) elongation

9. Wall thickness has minimal effect on surface roughness within the 1–7 mm range but significantly improves tensile strength and elongation beyond 7 mm (Figure 9).

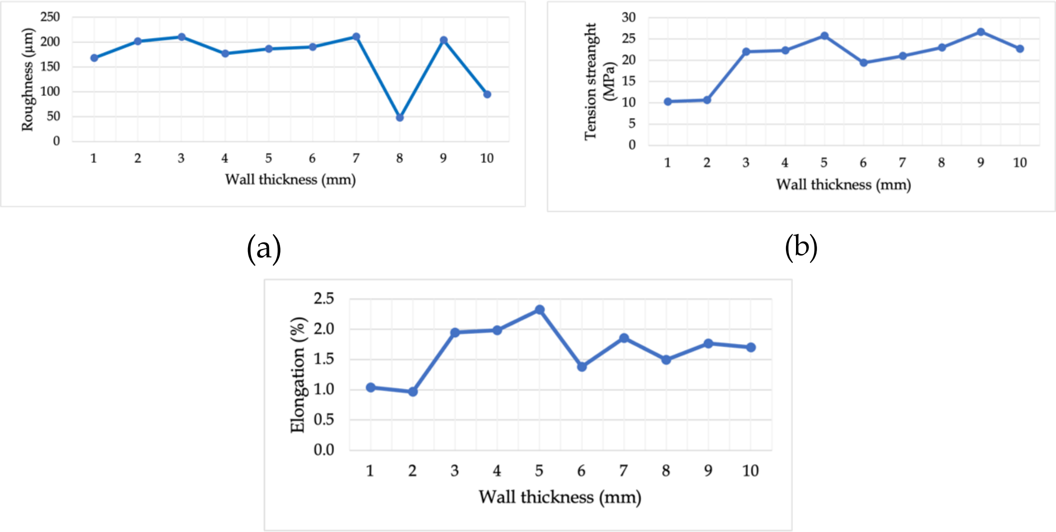

(a)

(b)

(c)

Figure 9. Effect of wall thickness on (a) surface roughness (b) tensile strength and (c) elongation

Optimization via Gray Relational Analysis identified the most favorable combination of input parameters as: 0.02 mm layer height, 9 mm wall thickness, 70% infill density, grid infill pattern, 215°C nozzle temperature, 75°C bed temperature, 40 mm/s print speed, PLA material, and 75% fan speed. This setting yielded the highest Gray Relational Grade (GRG) of 0.8685 (Run No. 9), representing the best balance among Ra, TS, and E.

Table 4. Gray relational coefficient with their grade and rank

Run No.	*Gray relational coefficient*			*Gray relational grade*	*Rank*
	Ra	*TS*	*E*		
1	0.9775	0.4648	0.8298	0.7573	6
2	0.9404	0.4400	1.0000	0.7935	3
3	0.9013	0.3626	0.6190	0.6277	18
4	0.7868	0.3793	0.5200	0.5621	31
5	0.7096	0.3402	0.5821	0.5440	33
6	0.8165	0.5593	0.7647	0.7135	9
7	0.8361	0.3976	0.9070	0.7136	8
8	1.0000	0.4177	1.0000	0.8059	2
9	0.9830	0.6226	1.0000	0.8685	1
10	0.9507	0.5789	0.8298	0.7865	4
11	0.7626	1.0000	0.5200	0.7609	5
12	0.7096	0.3976	1.0000	0.7024	11
13	0.6414	0.4400	0.9070	0.6628	14
14	0.4922	0.3708	0.6190	0.4940	40
15	0.4658	0.3793	0.7091	0.5181	39
16	0.6230	0.6226	0.5821	0.6092	22
17	0.5832	0.5410	0.7091	0.6111	21
18	0.7214	0.6000	0.9070	0.7428	7
19	0.7096	0.8049	0.6190	0.7112	10
20	0.7660	0.6735	0.6610	0.7002	12
21	0.6367	0.4400	0.8298	0.6355	16
22	0.5852	0.3976	0.7647	0.5825	28
23	0.4156	0.3793	0.6610	0.4853	47
24	0.3735	0.4783	0.6190	0.4903	42
25	0.3333	0.3626	0.4937	0.3965	50
26	0.5218	0.3882	0.9070	0.6057	23
27	0.5282	0.3976	0.8298	0.5852	27
28	0.6185	0.4648	0.7647	0.6160	20
29	0.5972	0.8462	0.4105	0.6180	19
30	0.6344	0.4177	1.0000	0.6840	13
31	0.5413	0.6226	0.5200	0.5613	32
32	0.5661	0.4783	0.7647	0.6030	24
33	0.4596	0.4648	1.0000	0.6415	15
34	0.3930	0.3708	0.5493	0.4377	49
35	0.3626	0.4074	0.5821	0.4507	48

36	0.5036	0.8049	0.4286	0.5790	29
37	0.4760	0.5593	0.7647	0.6000	25
38	0.5413	0.6000	0.6190	0.5868	26
39	0.5347	0.5238	0.5493	0.5359	37
40	0.5499	0.3333	0.5821	0.4884	45
41	0.4760	0.8919	0.3514	0.5731	30
42	0.4049	0.8462	0.3786	0.5432	34
43	0.3851	0.6471	0.5821	0.5381	35
44	0.3385	0.6471	0.9070	0.6309	17
45	0.3405	0.5077	0.7647	0.5376	36
46	0.3664	0.6471	0.4483	0.4873	46
47	0.4156	0.4177	0.7647	0.5327	38
48	0.4030	0.7021	0.3645	0.4899	43
49	0.4376	0.6735	0.3645	0.4918	41
50	0.4658	0.6226	0.3786	0.4890	44

DISCUSSION

The results underscore the multidimensional and interdependent nature of process parameters in Fused Deposition Modeling (FDM) 3D printing. Surface quality and mechanical integrity are strongly influenced not only by thermal and geometric settings but also by material selection and deposition strategy.

Layer height demonstrated a predictable increase in surface roughness due to the stair-stepping effect. However, the associated improvement in tensile strength and elongation at higher layer heights suggests improved interlayer bonding, possibly due to extended cooling intervals that allow for thermal diffusion and material coalescence (Zeng et al., 2022).

In contrast, fan speed demonstrates a more intricate influence. While its primary function is to enhance the solidification rate of extruded material, excessive cooling can impede interlayer adhesion, thereby compromising both mechanical strength and ductility (Vanaei & Elahinia, 2024). A comparable detrimental effect is observed at elevated printing speeds, where the reduced deposition time limits the thermal bonding interval, resulting in diminished structural integrity and flexibility (Yi et al., 2024).

Material analysis reveals the superior performance of PLA over ABS, aligning with previous studies that associate PLA's low viscosity and lower extrusion temperature with finer surface finishes and stronger mechanical properties (Mourya et al., 2024). However, the trade-off remains in PLA's lower thermal resistance, which may limit its applications in high-temperature environments (Xia et al., 2023).

Elevated bed temperatures were found to induce thermal expansion artifacts, thereby increasing surface roughness and reducing tensile properties—possibly due to microstructural defects or partial degradation (Shanmugam et al., 2024). Similarly, nozzle temperatures beyond 220°C led to over-extrusion and poor interlayer adhesion, corroborating the existence of an optimal processing window for thermal parameters.

Design-related parameters, including infill pattern and wall thickness, play a crucial role in influencing load transfer and stress dissipation within 3D-printed components. Among the tested configurations, the honeycomb infill pattern exhibited superior mechanical behavior, primarily due to its hexagonal lattice structure, which promotes uniform stress distribution under loading conditions (Nazari & Abedi, 2025). Additionally, increasing the wall thickness was found to substantially enhance both tensile strength and ductility, albeit with minimal impact on surface quality (Gordelier et al., 2019).

An intriguing observation emerged regarding the non-linear effect of infill density on surface quality. Specifically, moderate infill levels yielded superior surface finishes compared to both low and high extremes. This behavior is likely due to an optimal equilibrium between structural support and thermal regulation during the printing process. In contrast, excessively high infill densities may result in material over-deposition and localized heat build-up, negatively affecting surface integrity (Goh et al., 2018).

The optimization via Gray Relational Analysis provided a comprehensive framework for multi-criteria decision-making. The optimal configuration reflects a careful synergy between thermal, geometric, and material parameters. The high GRG score (0.8685) confirms that these parameter combinations effectively balance surface finish and mechanical performance, offering a reliable reference for high-quality, functional 3D printed components.

CONCLUSIONS AND RECOMMENDATIONS

This study successfully optimized the process parameters of FDM 3D printing to improve mechanical properties and surface quality using Gray Relational Analysis (GRA). The findings confirm that process parameter selection plays a decisive role in determining printed part quality. Among 50 test runs, the 9th experimental run achieved the highest GRG score of 0.8685, representing the best-performing configuration. The optimal parameter set includes: 0.02 mm layer height, 9 mm wall thickness, 70% infill density, grid infill pattern, 215°C nozzle temperature, 75°C bed temperature, 40 mm/s print speed, PLA material, and 75% fan speed.

This combination significantly improved both mechanical strength and surface finish, demonstrating practical implications for enhancing the reliability and quality of FDM-printed components. These findings offer a valuable reference for industrial practitioners and researchers aiming to optimize FDM settings in precision manufacturing applications. It is recommended that these parameter configurations be adopted as a guideline for similar material and machine conditions.

FURTHER STUDY

Despite the promising results, this study has limitations. The investigation focused solely on predefined parameter levels using open-source experimental data, without exploring dynamic or adaptive control during the printing process. Additionally, the material scope was limited to PLA and ABS, potentially restricting generalizability across different thermoplastics.

Future research should consider integrating real-time monitoring systems, exploring the impact of composite or advanced materials, and incorporating thermal and structural simulations to predict performance more accurately. Moreover, multi-objective optimization approaches combining GRA with other intelligent systems such as machine learning or evolutionary algorithms could further enhance the robustness and adaptability of FDM parameter optimization.

ACKNOWLEDGMENT

The author would like to express sincere gratitude to the Mechanical Engineering Study Program, Faculty of Engineering, Universitas Muhammadiyah Yogyakarta, for the invaluable support and facilities provided during this research.

REFERENCES

Chakraborty, S., Datta, H. N., & Chakraborty, S. (2023). Grey relational analysis-based optimization of machining processes: a comprehensive review. *Process Integration and Optimization for Sustainability*, *7*(4), 609-639.

Chen, X. (2023). Overview of Gray System Theory. In *Application of Gray System Theory in Fishery Science* (pp. 1-20). Springer.

Dev, S., & Srivastava, R. (2021). Effect of infill parameters on material sustainability and mechanical properties in fused deposition modelling process: a case study. *Progress in Additive Manufacturing*, *6*(4), 631-642.

Goh, G. D., Dikshit, V., Nagalingam, A. P., Goh, G. L., Agarwala, S., Sing, S. L., Wei, J., & Yeong, W. Y. (2018). Characterization of mechanical properties and fracture mode of additively manufactured carbon fiber and glass fiber reinforced thermoplastics. *Materials & Design*, *137*, 79-89.

Gordelier, T. J., Thies, P. R., Turner, L., & Johanning, L. (2019). Optimising the FDM additive manufacturing process to achieve maximum tensile strength: a state-of-the-art review. *Rapid Prototyping Journal*, *25*(6), 953-971.

Kechagias, J., & Zaoutsos, S. (2024). Effects of 3D-printing processing parameters on FFF parts' porosity: Outlook and trends. *Materials and Manufacturing Processes*, *39*(6), 804-814.

Khan, S., Joshi, K., & Deshmukh, S. (2022). A comprehensive review on effect of printing parameters on mechanical properties of FDM printed parts. *Materials Today: Proceedings*, *50*, 2119-2127.

Kumar, P., Gupta, P., & Singh, I. (2024). Optimisation of extrusion process parameters to make ABS-PC filament for 3D printing using Taguchi-GRA technique. *Advances in Materials and Processing Technologies*, *10*(3), 1921-1942.

Kumar, S., Singh, R., Singh, T., & Batish, A. (2023). Fused filament fabrication: A comprehensive review. *Journal of Thermoplastic Composite Materials*, *36*(2), 794-814.

Lee, S., Hwang, B., Lim, S., Yoon, S., Kim, T., Kim, K., Kim, D., & Park, C. (2019). Recent Trends and Prospects of 3D Content Using Artificial

Intelligence Technology. *Electronics and Telecommunications Trends*, *34*(4), 15-22.

Molero, E., Fernández, J. J., Rodríguez-Alabanda, O., Guerrero-Vaca, G., & Romero, P. E. (2020). Use of data mining techniques for the prediction of surface roughness of printed parts in polylactic acid (PLA) by fused deposition modeling (FDM): A practical application in frame glasses manufacturing. *Polymers*, *12*(4), 840.

Mourya, V., Bhore, S. P., & Wandale, P. G. (2024). Multiobjective optimization of tribological characteristics of 3D printed texture surfaces for ABS and PLA Polymers. *Journal of Thermoplastic Composite Materials*, *37*(2), 772-799.

Nazari, F., & Abedi, A. (2025). Investigating the effect of perforation geometry on the residual stress and mechanical behavior of 3D-printed honeycomb structure. *Multidiscipline Modeling in Materials and Structures*.

Patel, K., Acharya, S., & Acharya, G. (2024). Multi objective optimization of FDM parameters using taguchi grey relation analysis for PLA specimen. *Jurnal Kejuruteraan*, *36*(1), 113-122.

Raju, R., Varma, M. M. M., & Baghel, P. K. (2022). Optimization of process parameters for 3D printing process using Taguchi based grey approach. *Materials Today: Proceedings*, *68*, 1515-1520.

Shanmugam, V., Babu, K., Kannan, G., Mensah, R. A., Samantaray, S. K., & Das, O. (2024). The thermal properties of FDM printed polymeric materials: A review. *Polymer Degradation and Stability*, 110902.

Tamir, T. S., Xiong, G., Fang, Q., Yang, Y., Shen, Z., Zhou, M., & Jiang, J. (2023). Machine-learning-based monitoring and optimization of processing parameters in 3D printing. *International Journal of Computer Integrated Manufacturing*, *36*(9), 1362-1378.

Vanaei, S., & Elahinia, M. (2024). Applicable Materials and Techniques in 3D Printing. *Industrial Strategies and Solutions for 3D Printing: Applications and Optimization*, 43-57.

Xia, Y., Qian, S., Lu, W., Zhang, Z., Cheng, H., & Sheng, K. (2023). A strategy to prepare high-robust and ultra-tough polylactic acid/polycaprolactone/talc composites with thermo-resistance. *Polymer Composites*, *44*(12), 8750-8765.

Yi, N., Chen, Y., Shen, J., Davies, R., & Ghita, O. (2024). Correlation between interfacial bond strength and degree of healing in overprinting PAEK on CF/PAEK composites. *Composites Part A: Applied Science and Manufacturing*, *183*, 108217.

Zeng, S., You, G., Yao, F., Li, Q., Wang, L., & Cao, H. (2022). Coupling effect of bonding temperature and reduced interlayer thickness on the interface characteristics and quality of the diffusion-bonded joints of Zr alloys. *Journal of Materials Research and Technology*, *18*, 2699-2710.